Targeting DNA Mismatches with Rhodium Intercalators Functionalized with a Cell-Penetrating Peptide†

Jens Brunner and Jacqueline K. Barton*

Division of Chemistry and Chemical Engineering, California Institute of Technology, Pasadena, California 91125

Received June 15, 2006; Revised Manuscript Received August 10, 2006

ABSTRACT: Cell-penetrating peptides are widely used to deliver cargo molecules into cells. Here we describe the synthesis, characterization, DNA binding, and cellular uptake studies of a series of metal−peptide conjugates containing oligoarginine as a cell-penetrating peptide. D-Octaarginine units are appended onto a rhodium intercalator containing the sterically expansive chrysenequinone diimine (chrysi) ligand to form Rh(chrysi)(phen)(bpy)$^{3+}$-tethered oligoarginine conjugates, where the peptide is attached to the ancillary bpy ligand; some conjugates also include a fluorescein or thiazole orange tag. These complexes bind and with photoactivation selectively cleave DNA neighboring single-base mismatches. The presence of the oligoarginines is found to increase the nonspecific binding affinity of the complexes for both matched and mismatched DNA, but for these conjugates, photocleavage remains selective for the mismatched site, as assayed using both gel electrophoresis and mass spectrometry experiments. Significantly, the rhodium complex does not interfere with the delivery properties of the cell-penetrating peptide. Confocal microscopy experiments show rapid nuclear localization of the metal−peptide conjugates containing the tethered fluorescein. Mass spectrometry experiments confirm the association of the rhodium with the HeLa cells. These results provide a strategy for targeting mismatch-selective metal complexes inside cell nuclei.

Efficient and rapid delivery of diagnostic probes and drugs into a cell is crucial in disease detection and treatment. Many drug candidates and probe molecules fail because of insufficient cellular uptake. Only molecules with a narrow range of molecular weight and polarity are able to directly cross the plasma membrane by passive diffusion (*1*). To circumvent the cellular uptake problems, the physical properties of the agent must be optimized to achieve acceptable levels of passive entry into cells. An alternative strategy is to conjugate the agent to a molecular transporter; this strategy allows agents with a wide range of physical properties to enter cells (*2*). Such transporters include the cell-penetrating peptides (CPPs)[1] which are often derived from HIV Tat or from *Antennapedia* (*3*). A CPP, closely related structurally to the HIV Tat peptide, is the oligoarginine CPP. Cellular uptake studies of homopeptides consisting of seven to nine arginines show an even greater level of uptake compared to that of the Tat peptide itself (*4*).

In our laboratory, we have designed metallointercalators that target DNA base pair mismatches with high selectivity (*5*−*7*). Rhodium(III) complexes with sterically demanding ligands such as chrysenequinone diimine (chrysi) or benzo[*a*]phenazinequinone diimine (phzi) (*8*) are too expansive to insert easily within well-matched B-DNA and instead bind preferentially to thermodynamically destabilized mismatched sites. With photoactivation, the complexes furthermore promote strand breakage neighboring the mismatched site. Rh(bpy)$_2$chrysi^{3+}, for example, has been shown to be both a general and highly specific mismatch recognition agent (*6*). Upon photoactivation, the complex cleaves at more than 80% of mismatch sites in all possible single-base pair sequence contexts. Moreover, the complex has been demonstrated to recognize and photocleave a single-base mismatch in a 2725 bp linearized plasmid heteroduplex. These sterically demanding intercalators have proven to be useful in assays for single-nucleotide polymorphisms (*9*) and as diagnostic agents in probing deficiencies in mismatch repair (*8*).

Transition metal complexes have been increasingly explored as novel diagnostic and chemotherapeutic agents (*10*−*12*), but these applications require their ready uptake within the cell. Although there is an extensive history of biological activities associated with octahedral metal complexes (*13*), few studies have been carried out explicitly to explore their cellular uptake. In contrast, increasingly, experiments have been carried out to explore applications of metal complexes containing appended peptides. We have developed a family of metal−peptide conjugates of ruthenium and rhodium intercalators to explore DNA hydrolysis (*14*) and DNA cross-linking (*15*) and to enhance DNA sequence selectivity (*16*, *17*). Importantly, recently an organometallic compound has been conjugated to a nuclear localization peptide and was successfully delivered to the nucleus of cells (*18*).

Given the increasing utility of transition metal complexes for biological applications and, in particular, in targeting specific DNA sites, we became interested in exploring

† Financial support for this work from the National Institutes of Health (Grant GM33309 to J.K.B.) and a postdoctoral fellowship of the German Academic Exchange Service (to J.B.) are acknowledged.

* To whom correspondence should be addressed. E-mail: jkbarton@caltech.edu. Telephone: (626) 395-6075. Fax: (626) 577-4976.

[1] Abbreviations: CPP, cell-penetrating peptide; chrysi, chrysenequinone diimine; phzi, benzo[*a*]phenazinequinone diimine; bpy3C, 4-propionic acid-4′-methyl-2,2′-bipyridine; Pbf, 2,2,4,6,7-pentamethyldihydrobenzofuran-5-sulfonyl; Mtt, methyltrityl; ICP-MS, inductively coupled plasma mass spectrometry.

10.1021/bi061198o CCC: $33.50
Published on Web 09/19/2006

whether appending CPPs to the metal complex might enhance cellular uptake while maintaining the DNA recognition characteristics of the parent coordination complex. Here we present the synthesis, DNA binding studies, and cellular uptake properties of bulky rhodium intercalators functionalized with a CPP. If the mismatch-specific rhodium intercalators are to be applied in probing mismatch repair within the cell and in developing new diagnostics, then their functionalization to allow rapid cell entry would be advantageous. We find that the complexes functionalized with a basic CPP still promote site-specific cleavage at mismatched sites in duplex DNA. The presence of the appended peptide increases the level of nonspecific binding to DNA but does not alter the site specificity of the photoreaction. Moreover, the complexes, once functionalized, are rapidly taken up into the cell. The CPP efficiently delivers the mismatched complex to its target location.

EXPERIMENTAL PROCEDURES

Materials. All reagents and solvents were of the highest commercially available grades and were used as received without further purification. [Rh(bpy3C)(chrysi)(phen)]Cl_3 (bpy3C = 4-propionic acid-4′-methyl-2,2′-bipyridine), containing a pendant carboxylate for attachment of the peptide, was synthesized using the *o*-quinone condensation method analogous to the procedure described previously (*19*). The metal complex was characterized by ESI mass spectrometry, UV−vis spectroscopy, and ^{1}H NMR spectroscopy (Supporting Information).

Instrumentation. Electronic spectra were recorded on a Beckman DU 7400 UV−visible spectrophotometer (Beckman Coulter). Mass spectra were measured on an LCQ mass spectrometer with electrospray ionization or on a PerSeptive Biosystems Voyager-DE Pro instrument with 3-hydroxypicolinic acid for DNA and α-cyano-4-hydroxycinnamic acid for peptides as a matrix (positive modus). The irradiations for the photocleavage experiments were performed on a 1000 W Oriel Hg/Xe arc lamp (Oriel, Stamford, CT) with 320−440 nm light.

Synthesis of the Peptide Conjugates. Solid-phase bound and protected peptides were purchased from AnaSpec, Inc. (San Jose, CA); arginine was protected as its 2,2,4,6,7-pentamethyldihydrobenzofuran-5-sulfonyl derivative and lysine as its methyltrityl (Mtt) derivative. The acid-modified metal complexes were coupled to the free amines of the peptide by standard HOBT/HBTU activated coupling reactions (*20*). Undecanoic acid-modified thiazole orange was synthesized as described previously (*21*). The nonapeptide [D-Arg-$(Pbf)_8$Lys(Mtt)] was purchased on the solid support with N-terminal Fmoc groups already deprotected. The peptides were cleaved from the resin using 95% trifluoroacetic acid, 2.5% triisopropylsilane, and 2.5% water for 3 h at ambient temperature and then precipitated by addition of cold diethyl ether. In all cases, the final products were obtained in analytical purity using a HP1100 HPLC system fitted with a Vydac C18-packed reverse-phase column using a water (0.1% trifluoroacetic acid) (solvent A)/acetonitrile (solvent B) gradient and analyzed by ESI and MALDI-TOF mass spectrometry (Supporting Information). All conjugates employed in this study were used as their corresponding trifluoroacetate salts bearing a full complement of counterions. The concentrations of the bioconjugates were determined by their absorptions of fluorescein (ϵ = 67 000 M^{-1} cm^{-1} at 492 nm, pH 8) and thiazole orange (ϵ = 63 000 M^{-1} cm^{-1} at 500 nm) or the absorption of [Rh(bpy)(chrysi)(phen)]$^{3+}$ (ϵ = 9400 M^{-1} cm^{-1} at 389 nm).

DNA Preparation and Photocleavage Experiments. The oligonucleotides 5′-GGT AAT CCG TCA CCA TCG TGG GAC CGA CAT C-3′, 5′-GGT AAT CCG TCA CCA TCG TG*C* GAC CGA CAT C-3′, and 5′-GAT GTC GGT CCC ACG ATG GTG ACG GAT TAC C-3′, where *C* denotes the position of the mismatch, were synthesized on an ABI 392 DNA/RNA synthesizer (Applied Biosystems) by using standard phosphoramidite solid-phase synthesis. To cleave the oligonucleotides from the resin, the DNA was incubated in 30% aqueous ammonia for 16 h at 60 °C. The cleaved DNA strands were dried in a vacuum and resuspended in water prior to purification by HPLC. Following the first purification, the dimethoxytrityl group was removed with 80% acetic acid, and the strands were repurified by HPLC. MALDI-TOF mass spectrometry was used to characterize the strands.

For the MALDI-TOF mass spectrometric detection of the photocleavage experiments (*22*), the oligonucleotides were suspended in a buffer containing 50 mM NaCl and 10 mM sodium phosphate (pH 7.0) and quantified by UV−visible spectroscopy. DNA duplexes were annealed by combining an equal number of moles of the desired DNA complements in the buffer and heating at 90 °C for 5 min, followed by slow cooling to ambient temperature. To the annealed DNA was then added 1 equiv of rhodium complex modified with peptide, and the sample was irradiated for 15 min. After irradiation, all samples were worked up by the ZipTip procedure (Millipore, TN225 ziptip protocol), and MALDI-TOF mass spectra were measured with 3-hydroxypicolinic acid as the matrix.

For the detection of the photocleavage reaction by gel electrophoresis (*5*−*7*), the DNA single strands were 5′-labeled with [γ-^{32}P]ATP and T4 polynucleotide kinase. The labeled strands were further purified by gel electrophoresis (20% denaturing polyacrylamide gel), eluted from the gel by soaking in triethylammonium acetate (100 mM, pH 7), ethanol precipitated, and annealed in the presence of unlabeled DNA. To the duplex DNA was then added 1 equiv of rhodium complex modified with peptide, and the sample was irradiated. After irradiation, all samples were lyophilized, denaturing formamide loading dye was added, and the samples were electrophoresed on a 20% polyacrylamide denaturing gel. The photocleavage results were quantitated by phosphoimagery (PhosphorImager, Molecular Dynamics).

Cellular Uptake Experiments. The rhodium complex fluorescein-modified peptide **1** was dissolved in PBS buffer (pH 7.2), and the concentration was determined by absorption of fluorescein at 490 nm. HeLa cells (ATCC, CCL2) were grown in a solution of 89% minimal essential medium, 10% fetal bovine serum, and 1% penicillin−streptomycin (100×) (all Gibco) under an atmosphere of 5% CO_2 on glass-bottomed dishes (MatTek Corp., Ashland, MA), and each of these was used for cellular uptake experiments. Various amounts of peptide conjugates were added to approximately 10^4 cells in medium (combined total of 200 μL) and incubated for varying amounts of time at 37 °C. The cells were washed with PBS (2 × 200 μL), and then an additional 200 μL of PBS was added. Confocal microscopy was

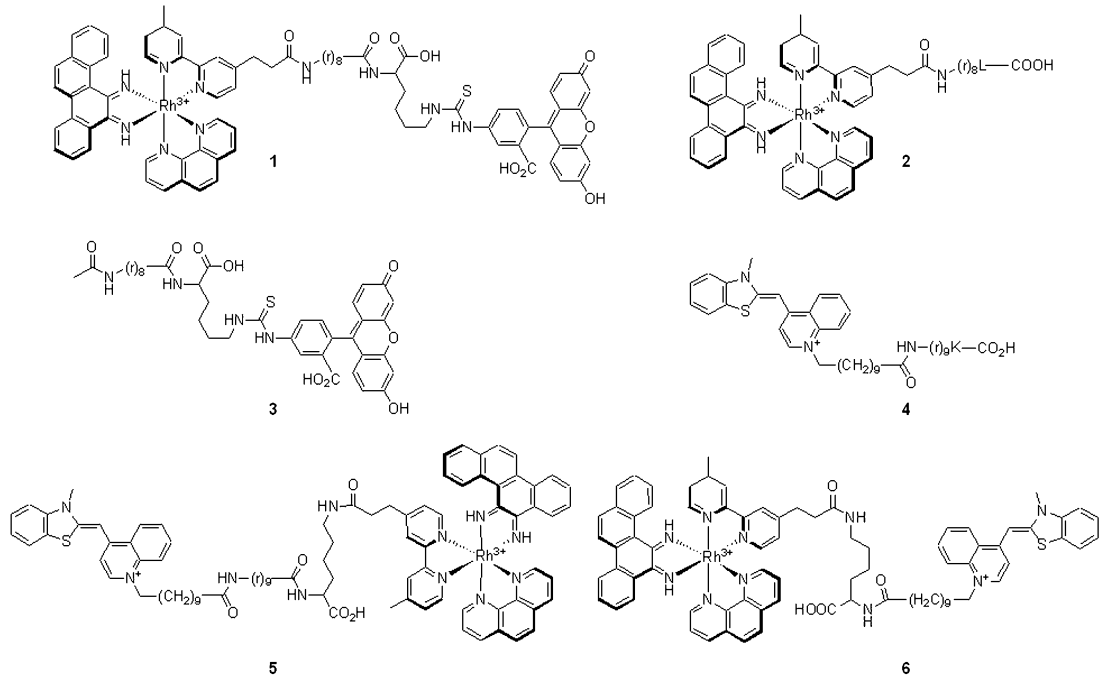

FIGURE 1: Chemical structures of the peptide conjugates.

performed on a Zeiss LSM Pascal inverted microscope using a planapochromate 63×/NA 1.4 oil immersion objective. The confocal microscope was equipped with an ArKr laser which was used to excite the dyes. The carboxyfluorescein was excited using the 488 nm laser line. Relative fluorescence was measured using the Zeiss 3D for LSM software.

Inductively Coupled Plasma Mass Spectrometric (ICP-MS) Detection of Rh. Rhodium conjugate **1** was dissolved in PBS buffer (pH 7.2), and the concentration was determined by absorption of fluorescein at 490 nm. HeLa cells (ATCC, CCL2), 10 000 per vial, were seeded in a 96-well plate in 200 μL of medium, consisting of a solution of 89% minimal essential medium, 10% fetal bovine serum, and 1% penicillin−streptomycin (100×) (all Gibco) under an atmosphere of 5% CO_2. After 24 h, the medium was replaced with fresh medium, and 9.9 μL of **1** (460 μM) in PBS, yielding a total concentration of 21 μM **1**, was added. After incubation for 1 h at 37 °C, the medium was collected, and cells were washed with 200 μL of PBS. The medium and the washing solution were combined and filled with water and HNO_3 to a total volume of 2.5 mL of 1% HNO_3. The washed cells were treated with 36 μL of HNO_3 (70%) for 1 h at room temperature and 1 h at 60 °C. After this, water was added to a total volume of 2.5 mL. The samples were then directly used for measuring the Rh content using ICP-MS on a Hewlett-Packard 4500 ICP-MS system.

RESULTS

Synthesis and Characterization of Peptide Conjugates. Conjugates **1**−**5**, as illustrated in Figure 1, all contain an oligoarginine that serves as a CPP and are either coupled both to a bulky metallointercalator and to a fluorophore, fluorescein, **1**, or thiazole orange, **5**, or coupled to the metal, **2**, or fluorophore, **3** and **4**, separately. Also prepared was the rhodium complex coupled to thiazole orange with an alkyl chain as a linker rather than an oligoarginine, **6**. The conjugates were synthesized as shown in Figure 2 by solid-phase chemistry. The carboxylic acid-modified rhodium complex was synthesized with a procedure analogous to that recently published (*19*), except bpy3C was used instead of bpy to provide a carboxylate for tethering of the conjugate. D-Arginines were chosen because they are more biostable than their L-isomers. The modifications were introduced into the N- and C-termini of the peptides so that the octaarginine peptide can act as a spacer and prevent possible quenching of the dyes by the metal complex (*23*).

As illustrated in Figure 2, the C-terminal modification was added to the peptide via a Mtt-protected lysine, which could be selectively deprotected. N-Terminal modifications were obtained by N-acylation of the N-terminal amine by the carboxylic acid-modified rhodium complex (**1** and **2**), acetic acid (**3**), or undecanoic acid-modified thiazole orange (**4**−**6**), which were preactivated by a HBTU/HOBT/DIEA mixture. Cleavage of the Mtt protecting group with 3% TFA in dichloromethane yields the free ϵ-amine at the lysine, which can then be further modified with the second group (fluorescein or Rh complex). Cleavage from the resin can be performed under standard Fmoc cleavage conditions, since the rhodium complexes are found to be stable under these conditions. The final products are further purified by reverse-phase HPLC and characterized by MALDI-TOF mass spectrometry. The conjugates can be quantified on the basis of their absorptions.

DNA Photocleavage of the Mismatch-Selective Conjugates. We were interested first in determining whether conjugation of the CPP peptide affects targeting of the bulky intercalator to the mismatched site. Mismatch selectivity is determined primarily through DNA photocleavage reactions. 5′-^{32}P-labeled double-stranded matched or mismatched oligonucleotides were incubated with Rh−peptide conjugate **1**, **2**, **5**, or **6** for 5 min and then irradiated for 15 min. The cleavage reaction was then analyzed by polyacrylamide gel electrophoresis (PAGE). Figure 3 shows PAGE analysis of a photocleavage reaction of 1 μM **1** and 1 μM duplex DNA **AB** containing a single CC mismatch. As is evident in Figure 3 for **1**, upon photoactivation of the Rh complex-modified

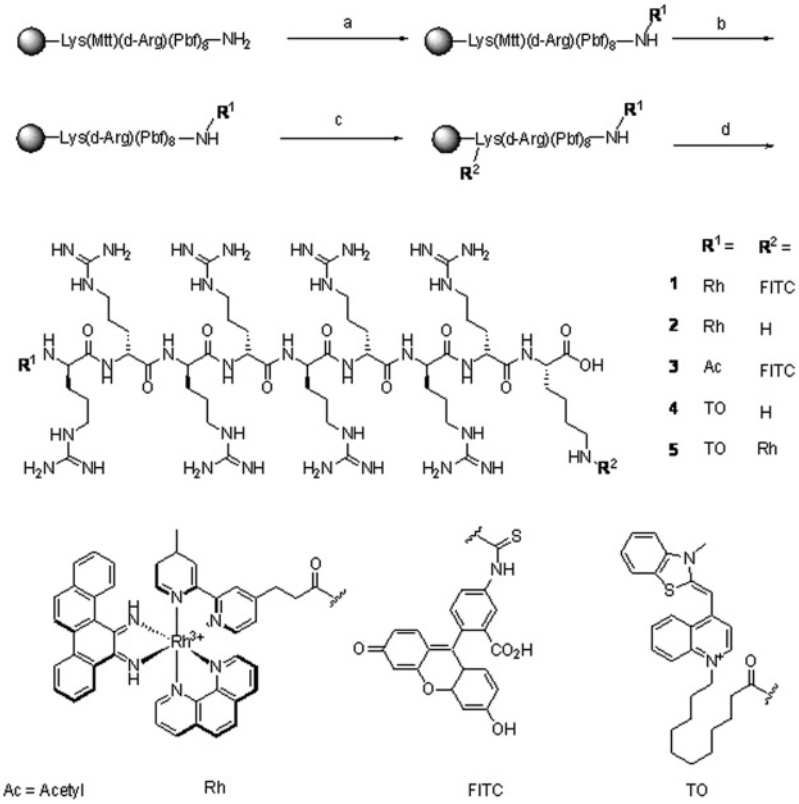

FIGURE 2: Strategy for the synthesis of conjugates **1**−**5**. The following reagents were utilized: (a) HOBT/HBTU, DIEA, R^1, DMF; (b) 3% TFA, DCM; (c) HOBT/HBTU, DIEA, R^2, DMF or FITC, DIEA, DMF; (d) 95% TFA, 2.5% TIS, 2.5% H_2O. Conjugate **6** was synthesized in an analogous procedure, using (Fmoc)Lys(Mtt) on the solid support instead of the peptide.

peptides, highly selective cleavage is observed, only on one strand, one base shifted to the 3′-side next to the mismatched site. Cleavage occurs at the same site as that of the parent $Rh(bpy)_2chrysi^{3+}$. Equivalent site-specific cleavage is evident with the other peptide conjugates, **2** and **5** (Supporting Information). Preferential cleavage is apparent also at this site with the conjugate lacking the oligoarginine linker, although with slightly less specificity. No cleavage is observed when the DNAs are irradiated in the absence of **1** (light control, LC) or as a mixture of **1** and mismatched DNA without irradiation (dark control, DC).

Also shown in Figure 3 are photocleavage studies performed with a matched oligonucleotide, **AC**, and the Rh−peptide conjugate, **1**. PAGE analysis of the photocleavage reaction shows no detectable DNA cleavage with fully matched DNA using any of the rhodium conjugates at concentrations of 0.01−20 μM Rh. It is therefore clear that tethering of the oligoarginine does not alter site-specific targeting of the bulky rhodium intercalator to the mismatched site by photocleavage.

The photocleavage reaction may also be analyzed by MALDI-TOF mass spectrometry (*22)*. As shown in Figure 4, the uncleaved DNAs and their doubly charged species are clearly apparent, as are cleavage products at *m*/*z* 5934.73 and *m*/*z* 3429.52, which correspond to the 3′- and 5′-phosphate-modified cleaved DNA products, respectively. These results are fully consistent with the photocleavage products seen by PAGE analysis. The cleavage occurs one base shifted toward the 3′-end next to the mismatched site, and cleavage is apparent only on the A strand after reaction with the **AB** mismatched duplex. It is interesting that we also observe a second cleavage product at *m*/*z* 3618.19 (M_{calc} = 3620.4), which we have assigned to the 2,3-dehydronucleotide of the cleaved DNA (*22*). No fragments are observed without irradiation (DC) or with irradiation but in the absence of **1** (LC) (Supporting Information).

It should be noted that MALDI-TOF mass spectrometric analysis shows also no cleavage with the fully matched duplex DNA **AC** (Supporting Information). The MALDI-TOF mass spectrometric analysis of the photocleavage reaction therefore fully confirms the highly selective photocleavage observed by PAGE analysis.

DNA Binding Assays. Given the presence of the appended oligoarginine units tethered to the metal complex, we were interested in determining the effect on DNA binding and selectivity. First, we examined the binding affinity of **1** for mismatched DNA **AB** in photocleavage titrations, where the yield of the photocleavage reaction with different amounts of DNA and rhodium peptide **1** is quantified by phosphoimagery. The ratio of **1** to mismatched DNA duplex at the photocleavage reaction was kept at 1:1. Figure 5 shows the corresponding binding isotherm after PAGE analysis and quantitation of the photocleavage reaction with different concentrations of **1** and the **AB** mismatched DNA. At high concentrations, significant scatter is evident, precluding a quantitative determination. From these data, we may estimate, however, that the constant for binding of **1** to mismatched DNA **AB** is $\geq 3 \times 10^7$ M^{-1} for the CC mismatch in 50 mM NaCl and 10 mM phosphate at 20 °C. This lower estimate corresponds to an increase of at least 2 orders of magnitude compared to the determined binding affinity of the parent $Rh(bpy)_2chrysi^{3+}$ not modified with a cationic peptide (*7*).

Photocleavage studies were also performed with conjugates **2**, **5**, and **6**. These conjugates all exhibit selective photo-

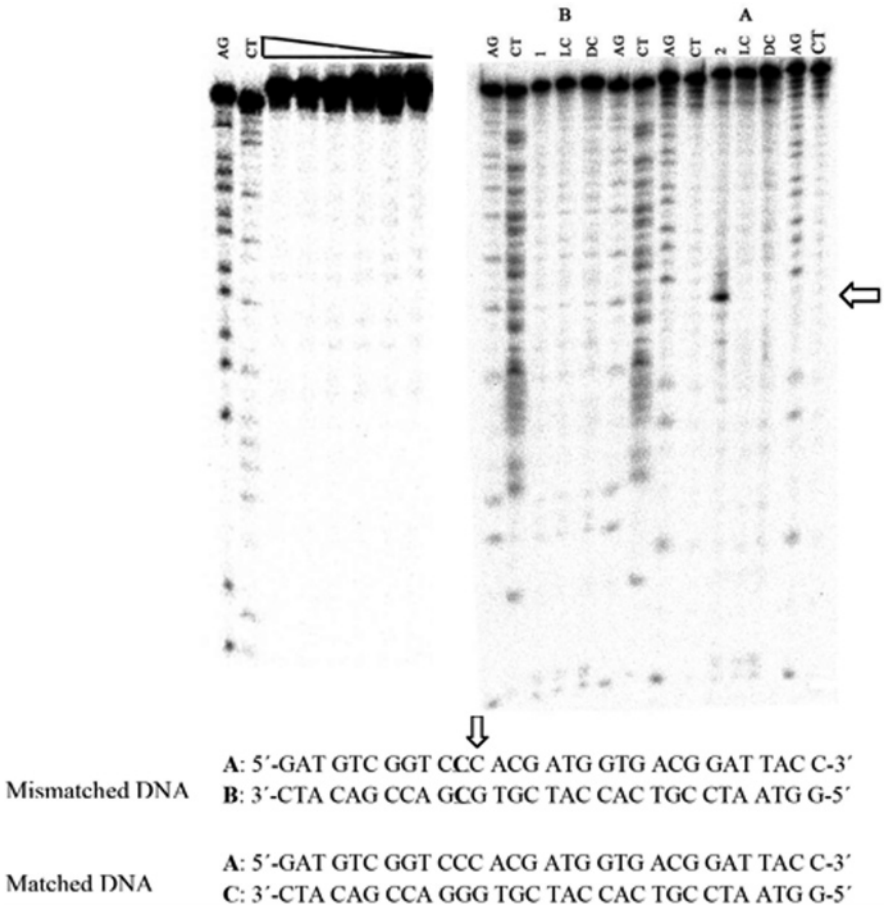

FIGURE 3: Site-specific photocleavage neighboring a DNA mismatch with the metal−peptide conjugate, **1**. Below are shown the DNA sequences utilized for mismatched DNA, strands labeled **A** and **B**, and matched DNA, strands **A** and **C**, with the CC mismatch in bold and the site of cleavage, neighboring the mismatch, denoted with an arrow. Above is the phosphoimagery of 20% denaturing polyacrylamide gels for photocleavage in 10 mM phosphate and 50 mM NaCl (pH 7) on **AC** (left) and **AB** (right). Shown (left) is the phosphoimagery after denaturing PAGE of 0.01−20 μM **1** and matched DNA **AC**, where strand **A** was ^{32}P-5′-end-labeled. Shown (right) is the phosphoimagery after denaturing PAGE of 1 μM complex **1** and mismatched DNA **AB**, where for **A**, DNA strand **A** was ^{32}P-5′-end-labeled and for **B**, DNA strand **B** was ^{32}P-5′-end-labeled. On the right, selective photocleavage is evident on DNA strand **A**, also denoted with an arrow, by the rhodium peptide complex, **1**, neighboring the mismatched site, while on the left, no photocleavage is seen. AG and CT lanes indicate Maxim−Gilbert sequencing reactions; LC lanes indicate the light control sample irradiated without metal complex, and DC lanes indicate the dark control incubated with the metal complex but without light.

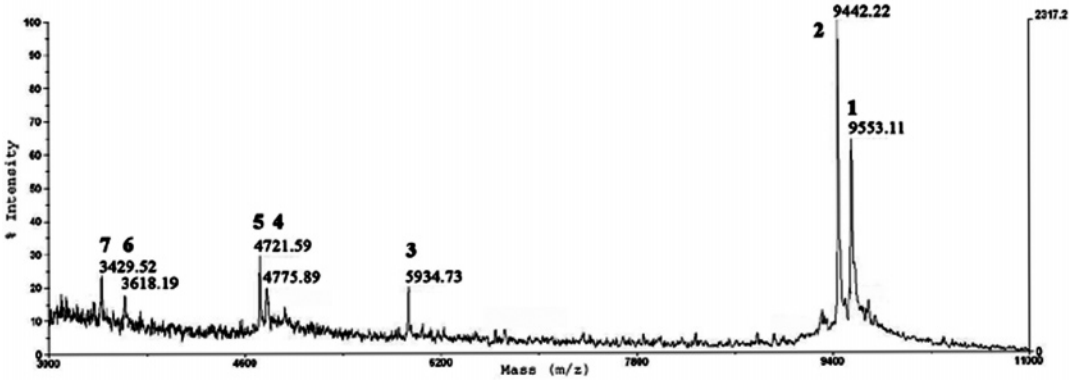

FIGURE 4: MALDI-TOF mass spectrum after DNA photocleavage by conjugate **1**. The photocleavage conditions were 1 μM **1** and 1 μM mismatched DNA **AB** in 50 mM NaCl and 10 mM sodium phosphate (pH 7) with irradiation for 15 min. The cleavage products are marked with numbers. The uncleaved DNAs, **1** and **2**, correspond to ions at *m*/*z* 9553.11 (M_{calc} = 9553.2) and *m*/*z* 9442.22 (M_{calc} = 9442.2) with their double-charged species, **4** and **5**, at *m*/*z* 4775.89 (M_{calc} = 4777.1) and *m*/*z* 4721.59 (M_{calc} = 4721.6). Cleavage products **3** at *m*/*z* 5934.73 (M_{calc} = 5934.9) and **7** at *m*/*z* 3429.52 (M_{calc} = 3430.2) can be observed, which correspond to the 3′- and 5′-phosphate-modified cleaved DNA products. Site-specific cleavage is observed only on strand **A** neighboring the mismatch. The cleavage occurs 1 base shifted toward the 3′-end next to the mismatched site. At *m*/*z* 3618.19 (M_{calc} = 3620.4), a second cleavage product, **6**, is found which we assign to the 2,3-dehydronucleotide of the cleaved DNA.

cleavage at the same site as **1**. In fact, photocleavage is observed with **2** and **5** at lower DNA and peptide concentrations than with **1**. On the basis of relative photocleavage, we estimate that the relative binding affinities for the mismatched site increase for the complexes in the following order: **6** < **1** < **2** < **5**. Clearly, the cationic oligoarginine

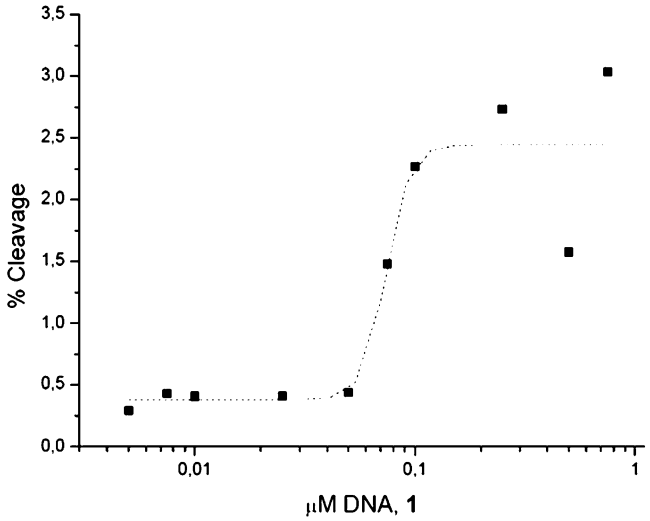

FIGURE 5: Binding isotherm for **1** targeted to oligonucleotide **AB** containing a CC mismatch. Photocleavage reactions were performed with 0.005−0.75 μM **1** and 0.005−0.75 μM mismatched DNA **AB** in 50 mM NaCl and 10 mM sodium phosphate (pH 7) and irradiation for 15 min. Quantitation was performed by phosphoimagery after PAGE analysis as described for Figure 3. The percent cleavage corresponds to cleavage at the mismatched site normalized to total counts within the lane.

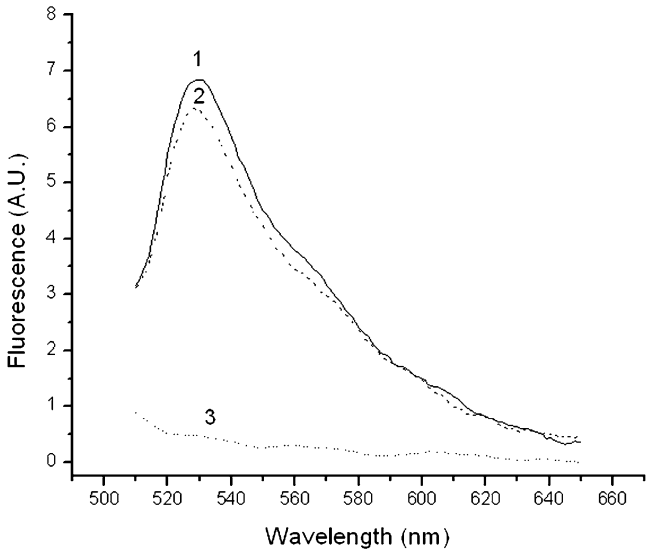

FIGURE 6: Fluorescence, *F* (arbitrary units), of metal−peptide conjugate **5** (0.1 μM) with mismatched DNA (**1**), with matched DNA (**2**), and without DNA (**3**) in 50 mM NaCl and 10 mM phosphate (pH 7); the excitation wavelength was 500 nm. The oligonucleotides that were used at 0.1 μM are as described in the legend of Figure 3.

and, to a lesser extent, the cationic thiazole orange enhance binding affinity; the oligoarginine and thiazole orange moieties understandably contribute to overall DNA binding. The fluorescein moiety, on the other hand, decreases the affinity.

The binding to DNA of the peptides modified with thiazole orange, **4**−**6**, can be monitored also by fluorescence spectroscopy. Thiazole orange is not fluorescent in the absence of DNA but fluoresces brightly in the presence of DNA (*24*). Figure 6 shows the fluorescence increase that is observed after addition of 0.1 μM mismatched DNA **AB** or matched DNA **AC** to a solution of 0.1 μM **5**. Interestingly, no appreciable difference in fluorescence between matched and mismatched DNA is observed, yet under comparable conditions, photocleavage is evident only on mismatched **AB** and not on the well-matched duplex **AC**.

These experiments indicate that nonspecific binding does occur with duplex DNA for the metal peptides containing the cationic CPP. It is perhaps not surprising that an electrostatic association is evident for the cationic peptides with the DNA polyanion, yet this nonspecific interaction is not sufficient to orient the bulky chrysi intercalator inside a base pair binding site for strand cleavage. The photocleavage reaction requires a close, intercalative association for reaction, and this is evident only with the mismatched duplex. Fluorescence monitoring of the pendant thiazole orange does not reveal this difference, but it does reveal nonspecific association of the conjugates with the duplex.

*Cellular Uptake of Conjugates **1** and **3***. Cellular uptake of fluorescein-modified compounds **1** and **3** in live HeLa cells was studied by confocal laser scanning microscopy. As expected, HeLa cells incubated with 5 μM conjugate **3** for 60 min at 37 °C exhibit an uneven distribution of **3**, with very strong fluorescence apparent in the nucleus (Figure 7). Importantly, with 5 μM **1**, containing the CPP appended onto the bulky rhodium intercalator, as also shown in Figure 6, similar results are obtained. For **1**, fast and efficient cellular uptake is evident with stronger fluorescence apparent in the nucleus. In fact, for both **1** and **3**, as quickly as the confocal microscopy can be performed, strong fluorescence is found in the nucleus of HeLa cells. The incorporation of the metal complex moiety onto the fluorescein-modified peptide appears to have no significant influence on the cell penetrating properties of the peptide.

Given the parallel behavior of **1** and **3**, we wanted also to explore uptake by assaying rhodium directly. This assay allows us to test whether the complex is decomposing in a manner where the rhodium complex is shed from the CPP. To estimate the amount of the Rh conjugate taken up by the HeLa cells, ICP-MS detection of rhodium was employed. After treatment of HeLa cells for 1 h with 20 μM **1** at 37 °C, ICP-MS measurements of solutions obtained from cell-bound and free Rh show 7.8 ± 0.7 ppb of the Rh conjugate associated with the cells and 231 ± 35.4 ppb of Rh still in the medium. If we assume an average cell volume of 1 pL (*25*) and therefore a total cell volume of 10 nL (10 000 cells), then the cell-bound Rh concentration is approximately 8 mM, where the medium Rh concentration is ∼11 μM; the metal−peptide conjugate appears to be concentrated within the cell. It should be noted, however, that this is at best a crude approximation. These data only indicate rhodium associated with the cells, not within the interior. It is instead the confocal microscopy data that establish nuclear uptake by the conjugates. The ICP-MS data, however, certainly support the idea that it is the intact metal−peptide conjugate that is incorporated.

DISCUSSION

With the overall goal of exploring biological activities of our coordination complexes that are selective for DNA mismatches, we were interested in finding a reliable way to bring these complexes inside cells. It should be noted that coordinatively saturated octahedral complexes containing the bpy ligand and derivatives are taken up inside cells without

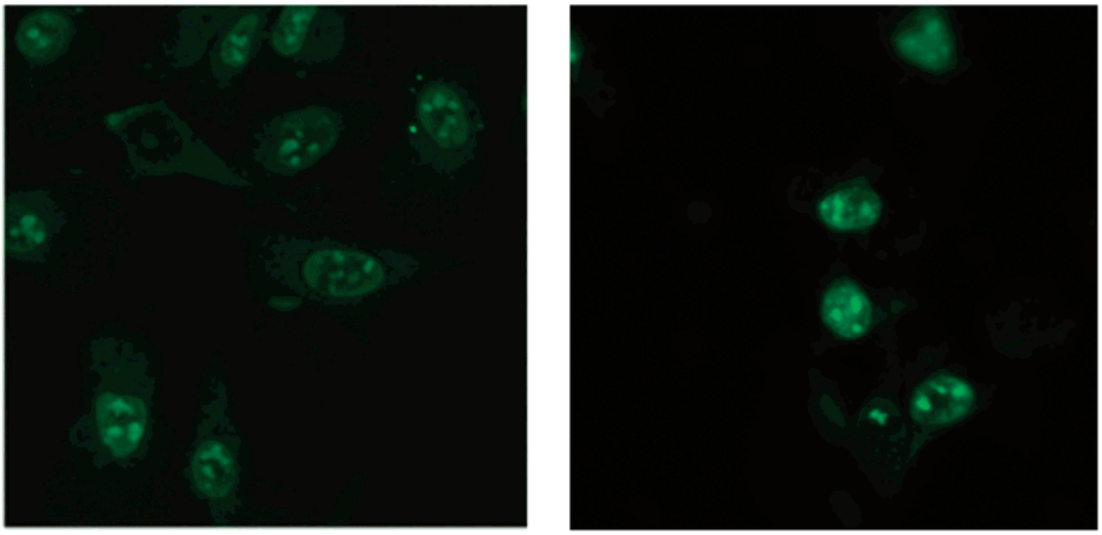

FIGURE 7: Confocal microscopy of HeLa cells treated with peptide conjugates. Shown are fluorescence images of HeLa cells after incubation for 60 min with 5 μM **3** (left) or **1** (right) at 37 °C. The excitation wavelength was 488 nm.

the need of the appended peptide (*13*; C. Puckett, unpublished results), but attachment of the CPP potentially offers a dependable means of delivering metal complexes to the nucleus. We therefore attached the mismatch-selective Rh(bpy)(chrysi)(phen)$^{3+}$ complex to D-octaarginine, which is a well-known cell-penetrating peptide that can act as a vehicle for delivery to the nucleus (*3*, *4*).

Rh(bpy)$_2$chrysi^{3+} is known to recognize and with photoactivation to cleave single-base mismatches within duplex DNA (*5*−*7*). An important issue in appending an extended functionality onto the metal complex scaffold is whether the peptide would alter the mismatch targeting properties of the metal complex. Using photocleavage as a probe, it is clear that the complex containing the tethered peptide still cleaves site-specifically neighboring the mismatch. In fact, MALDI-TOF mass spectrometry reveals that the photocleavage products are identical to those of the parent, with cleavage only on one strand and shifted to the 3′-side of the mismatch. These similar features of the metal−peptide conjugate and parent metal complex suggest that the orientation of the metal complex at its binding site is maintained in the conjugate.

There are important differences between the conjugate and parent metal complex, however. Photocleavage titrations as a function of concentration allow the estimation of the binding affinity of the complex for its target site. Not surprisingly, we find that appending the cationic oligoarginines increases the binding affinity for the DNA polyanion by at least 2 orders of magnitude. Moreover, utilizing an additionally appended thiazole orange as a fluorescent probe reveals that the electrostatic interactions of the oligoarginine with DNA, coupled with the noncovalent association of the thiazole moiety, lead to an appreciable nonspecific binding of the conjugate to well-matched as well as mismatched DNA. This nonspecific binding does not, however, yield a productive site-specific photoreaction. Thus, while the appended peptide does enhance nonselective binding, it does not interfere with mismatch-specific targeting by photocleavage.

Significantly, the presence of the bulky octahedral metal complex does not affect the delivery properties of the appended cell-penetrating peptide. Confocal microscopy shows rapid and efficient concentration of the conjugate containing the metal complex tethered to the CPP in the nucleus of HeLa cells. Moreover ICP-MS confirms that the rhodium complex is taken up by the cells. The bulky rhodium complex, despite its large size (11.3 Å diameter) and charge, does not appear to hinder transport across either the cell or nuclear membrane.

These results therefore establish a clear strategy for targeting octahedral metal complexes inside cells. Tethering of an octaarginine as a CPP onto an ancillary ligand of the metal complex offers a reliable means of intracellular delivery while maintaining, at least for the bulky metallointercalators, the targeting of mismatched DNA sites. This strategy now offers a route for exploring the biological activity of these complexes inside cells.

SUPPORTING INFORMATION AVAILABLE

Synthesis and characterization of the parent metal complex and complex conjugates as well as DNA photocleavage experiments and controls analyzed by gel electrophoresis and MALDI-TOF mass spectrometry for all the metal−peptide conjugates. This material is available free of charge via the Internet at http://pubs.acs.org.

REFERENCES

1. Lipinsky, C. A., Lombardo, F., Dominy, B. W., and Feeney, P. J. (2001) Experimental and computational approaches to estimate solubility and permeability in drug discovery and development settings, *Adv. Drug Delivery Rev. 46*, 3−26.
2. Fischer, R., Fotin-Mleczek, M., Hufnagel, H., and Brock, R. (2005) Break on through to the other side: Biophysics and cell biology shed light on cell-penetrating peptides, *ChemBioChem 6*, 2126−2142.
3. Magzoub, M., and Gräslund, A. (2004) Cell-penetrating peptides: Small from inception to application, *Q. Rev. Biophys. 37*, 147−195.
4. Wender, P. A., Mitchell, D. J., Pattabiraman, K., Pelkey, E. T., Steinman, L., and Rothbard, J. B. (2000) The design, synthesis, and evaluation of molecules that enable or enhance cellular uptake: Peptoid molecular transporters, *Proc. Natl. Acad. Sci. U.S.A. 97*, 13003−13008.
5. Jackson, B. A., and Barton, J. K. (1997) Recognition of DNA base mismatches by a rhodium intercalator, *J. Am. Chem. Soc. 119*, 12986−12987.

6. Jackson, B. A., Alekseyev, V. Y., and Barton, J. K. (1999) A versatile mismatch recognition agent: Specific cleavage of a plasmid DNA at a single base mispair, *Biochemistry 38*, 4655−4662.
7. Jackson, B. A., and Barton, J. K. (2000) Recognition of base mismatches in DNA by 5,6-chrysenequinone diimine complexes of rhodium(III): A proposed mechanism for preferential binding in destabilized regions of the double helix, *Biochemistry 39*, 6176−6182.
8. Junicke, H., Hart, J. R., Kisko, J., Glebov, O., Kirsch, I. R., and Barton, J. K. (2003) A rhodium(III) complex for high affinity DNA base pair mismatch recognition, *Proc. Natl. Acad. Sci. U.S.A. 100*, 3737−3742.
9. Hart, J. R., Johnson, M. D., and Barton, J. K. (2004) Single nucleotide polymorphism discovery by targeted DNA photocleavage, *Proc. Natl. Acad. Sci. U.S.A. 126*, 14040−14044.
10. Erkkila, K. E., Odom, D. T., and Barton, J. K. (1999) Recognition and reaction of metallointercalators with DNA, *Chem. Rev. 99*, 2777−2795.
11. Jamieson, E. R., and Lippard, S. J. (1999) Structure, recognition, and processing of cisplatin-DNA adducts, *Chem. Rev. 99*, 2467−2498.
12. Bednarski, P. J., Grunert, R., Zielzki, M., Wellner, A., Mackay, F. S., and Sadler, P. J. (2006) Light-activated destruction of cancer cell nuclei by platinum diazide complexes, *Chem. Biol. 13*, 61−67.
13. Dwyer, F. P., and Gyarfas, E. C. (1952) Biological activity of complex ions, *Nature 170*, 190−191.
14. Copeland, K. D., Fitzsimons, M. P., Houser, R. P., and Barton, J. K. (2002) DNA hydrolysis and oxidative cleavage by metal-binding peptides tethered to rhodium intercalators, *Biochemistry 41*, 343−356.
15. Copeland, K. D., Lueras, A. M. K., Stemp, E. D. A., and Barton, J. K. (2002) DNA crosslinking with metallointercalator-peptide conjugates, *Biochemistry 41*, 12785−12797.
16. Hastings, C. A., and Barton, J. K. (1999) Perturbing the DNA sequence selectivity of metallointercalator-peptide conjugates by single amino acid modification, *Biochemistry 38*, 10042−10051.
17. Sardesai, N. Y., Zimmermann, K., and Barton, J. K. (1994) DNA recognition by peptide complexes of rhodium(III): Example of a glutamate switch, *J. Am. Chem. Soc. 116*, 7502−7508.
18. Noor, F., Wüstholz, A., Kinscherf, R., and Metzler-Nolte, N. (2005) A cobaltocenium-peptide bioconjugate shows enhanced cellular uptake and directed nuclear delivery, *Angew. Chem., Int. Ed. 44*, 2429−2432.
19. Mürner, H., Jackson, B. A., and Barton, J. K. (1998) A versatile approach to rhodium(III) diimine metallointercalators: Condensation of ortho-quinones with coordinated cis-ammines, *Inorg. Chem. 37*, 3007−3012.
20. Brunner, J., Mokhir, A., and Kraemer, R. (2003) DNA-templated metal catalysis, *J. Am. Chem. Soc. 125*, 12410−12411.
21. Carreon, J. R., Mahon, K. P., Jr., and Kelley, S. O. (2004) Thiazole orange-peptide conjugates: Sensitivity of DNA binding to chemical structure, *Org. Lett. 6*, 517−519.
22. Brunner, J., and Barton, J. K. (2006) Site-specific DNA photocleavage by rhodium intercalators analyzed by MALDI-TOF mass spectrometry, *J. Am. Chem. Soc. 128*, 6772−6773.
23. Zeglis, B. M., and Barton, J. K. (2006) A mismatch-selective bifunctional rhodium-oregon green conjugate: A fluorescent probe for mismatched DNA, *J. Am. Chem. Soc. 128*, 5654−5655.
24. Nygren, J., Svanvik, N., and Kubista, M. (1998) The interactions between the fluorescent dye thiazole orange and DNA, *Biopolymers 46*, 39−51.
25. Chen, I., Horwarth, M., Lin, W., and Ting, A. Y. (2005) Site-specific labeling of cell surface proteins with biophysical probes using biotin ligase, *Nat. Methods 2*, 99−104.

BI061198O